



# Mechanical and thermoelectric properties of FeVSb-based half-Heusler alloys



A. El-Khouly<sup>a,b,\*</sup>, A.M. Adam<sup>c,d</sup>, E.M.M. Ibrahim<sup>c</sup>, Ayman Nafady<sup>e</sup>, D. Karpenkov<sup>f</sup>, A. Novitskii<sup>a</sup>, A. Voronin<sup>a</sup>, V. Khovaylo<sup>a</sup>, E.M. Elsehly<sup>a,b</sup>

<sup>a</sup> National University of Science and Technology MISIS, Moscow 119049, Russian Federation

<sup>b</sup> Physics Department, Faculty of Science, Damanhour University, 22516 Damanhour, Egypt

<sup>c</sup> Physics Department, Faculty of Science, Sohag University, 82524 Sohag, Egypt

<sup>d</sup> Faculty of Engineering, King Salman International University, Sinai, Egypt

<sup>e</sup> Department of Chemistry, College of Science, King Saud University, Riyadh 11451, Saudi Arabia

<sup>f</sup> Moscow State University, 119991 Moscow, Russian Federation

## ARTICLE INFO

### Article history:

Received 12 May 2021

Received in revised form 15 July 2021

Accepted 22 July 2021

Available online 24 July 2021

### Keywords:

Thermoelectric performance  
Half-Heusler alloys

Vickers hardness

Fracture toughness

Phonon scattering

Thermal conductivity

## ABSTRACT

Half Heusler FeVSb-based compounds are recently identified as promising thermoelectric materials for medium to high temperature range. In this research article, thermoelectric properties of half Heusler  $\text{FeV}_{1-x-y-z}\text{Hf}_x\text{Ti}_y\text{Nb}_z\text{Sb}$  and FeVSb samples were studied over a temperature range from 300 to 800 K. Transition heavy elements such as Hf, Ti and Nb were used as dopants to enhance the phonon scattering aiming at reducing the material's thermal conductivity. The  $\text{FeV}_{0.24}\text{Nb}_{0.4}\text{Hf}_{0.16}\text{Ti}_{0.2}\text{Sb}$  compound showed the lowest lattice thermal conductivity ( $\kappa_l$ ) with a value of  $(1.81 \pm 0.1 \text{ W m}^{-1} \text{ K}^{-1})$  at room temperature with a reduction of ~82% compared with that of FeVSb compound. A maximum power factor value of  $(9.8 \pm 0.9) \mu\text{W cm}^{-1} \text{ K}^{-2}$  at 800 K and figure of merit ( $zT$ ) value of 0.44 were recorded at 725 K for  $\text{FeV}_{0.24}\text{Nb}_{0.4}\text{Hf}_{0.16}\text{Ti}_{0.2}\text{Sb}$ . Vickers hardness method was used to estimate the hardness of the concerned alloys by micro-hardness technique, subjected to various applied loads. All the concerned samples showed significant mechanical stability. A maximum hardness value of  $19.15 \pm 0.77 \text{ GPa}$  at load of 0.98 N was obtained for the  $\text{FeV}_{0.24}\text{Nb}_{0.4}\text{Hf}_{0.16}\text{Ti}_{0.2}\text{Sb}$  compound.

© 2021 Elsevier B.V. All rights reserved.

## 1. Introduction

Numerous investigations showed that a good thermoelectric (TE) material is a narrow-gap semiconductor with a high electrical conductivity and a low thermal conduction. A mathematical expression called the TE figure of merit ( $zT$ ) was introduced to describe how a TE material is efficient. It is expressed as  $zT = S^2\sigma T/(\kappa_t)$ , where  $S$  refers to the Seebeck coefficient,  $\sigma$ , and  $\kappa_t$  are the material's electrical and thermal conductivity, respectively, while  $T$  is the absolute temperature. It was found that parameters  $S$  and  $\sigma$ , which tend to manifest an inverse relationship, strongly depend on the doping level and the chemical composition. Optimization of the doping level and the chemical composition are quite important for obtaining better thermoelectric performance. According to many previous reports, the product,  $S^2\sigma$ , which is known as the power factor  $PF$ , can be maximized by doping to attain the semiconductor-to-semimetal

transition. Whilst the thermal conductivity ( $\kappa_t$ ) can often be modified by chemical substitutions and doping [1,2].

However, optimization is very difficult problem, as the best thermoelectric material would behave as a "phonon-glass, electron-crystal" material [3]. That is, the materials would have the thermal properties of a glass and the electronic properties of a crystal.

Despite the intensive work to improve the performance of the well-known TE alloys, researchers have also been investigating other alloys and compounds and exploring new systems as potential TE materials. Applicable TE materials should be simple to synthesize and process. Also, their electronic and lattice properties should be conveniently tuned. Moreover, they should be chemically and thermally stable when used at high temperatures.

Due to their interesting electrical transport properties and their rich elemental combinations, half-Heusler (HH) alloys have attracted great research attention. In the field of energy conversion, HH alloys emerged recently among numerous thermoelectric materials as promising candidate. HH and related compounds are explored as a new class of thermoelectric materials and have shown a great

\* Corresponding authors.

E-mail addresses: [a.elhuli@misis.ru](mailto:a.elhuli@misis.ru), [menaim.elkhouly@yahoo.com](mailto:menaim.elkhouly@yahoo.com) (A. El-Khouly).

promise for efficient TE materials [4]. It was reported that HH alloys have high Seebeck coefficient  $\sim 100 \mu\text{V K}^{-1}$  at room temperature, which is the key feature for their high TE efficiency [5]. To fabricate efficient TE devices, both excellent n-type and p-type TE materials with high energy conversion efficiency and similar physical properties are required [6].

Although huge research efforts have been focused on enhancing the TE performance of n-type HH alloys, investigating p-type alloys is quite important as well. However, the reported work on p-type HH alloys is very few, hence, exploring potential p-type HH alloys or improving the performance of existing p-type HH alloys is significantly important.

Amongst the HH compounds, FeVSb is reported as a moderate temperature TE system, however, a few research works had been done on this system. Despite the high Seebeck coefficient and electrical conductivity of FeVSb, its high thermal conductivity is the main obstacle for the system to exhibit high TE performance [7]. As reported, the FeVSb HH system has thermal conductivity values in the range of  $10\text{--}13 \text{ W m}^{-1} \text{ K}^{-1}$  at room temperature [8]. Such values are very high to be used in TE applications or devices. Reduction of thermal conductivity in HH structures can be obtained by doping. It is worth to note that many previous reports studied the thermoelectric and mechanical properties of pure and doped FeVSb. For example, Huang et al. investigated the thermoelectric performance of FeVSb and n-type V ( $\text{Fe}_{1-x}\text{Cox}$ )Sb half-Heusler compounds [9,10]. The mechanical properties, in terms of elastic constants, of cubic FeVSb in a pressure ranging from 0 to 120 GPa was presented by Bo Kong et al. [11].

The current research article presents a study on thermoelectric and mechanical properties of FeVSb doped with heavy elements as Hf, Ti and Nb. Dopants are employed to enhance the phonon scattering aiming at reducing the material's thermal conductivity.  $\text{FeV}_{1-x-y-z}\text{Hf}_x\text{Ti}_y\text{Nb}_z\text{Sb}$  HH alloys were prepared by arc melting followed by induction melting. The prepared materials are characterized by X-ray diffraction (XRD) and Scanning electron microscopy (SEM) analysis while their transport thermoelectric properties are studied as a function of temperature from 300 to 800 K.

## 2. Experimental work

Ingots of  $\text{FeV}_{1-x-y-z}\text{Hf}_x\text{Ti}_y\text{Nb}_z\text{Sb}$  were synthesized from pure elements of Fe (rod, 99.99%), V (piece, 99.99%), Hf (rod, 99.99%), Ti (rod, 99.99%), Nb (pieces, 99.99%) and Sb (block, 99.999%) at various composition ratios by arc melting followed by induction melting. About 3 wt% Sb excess was added to the alloy mixture to compensate the possible Sb evaporation during high-temperature processing. The ingots were sealed in evacuated quartz tubes and annealed at 923 K for 48 h. Then, the samples were milled into fine powders and consolidated with the spark plasma sintering (SPS) system (Labox 650, Sinter-Land, Japan) at 1023 K for 15 min under a uniaxial pressure of 65 MPa in vacuum. The obtained consolidated disks were annealed at 923 K for 3 days to promote ordering of the crystal structure. Equipment used for analysis, scientific instruments, equations and more details related to the thermoelectric measurements can be found elsewhere [12]. Hardness is an important mechanical property to characterize a material. The Vickers hardness ( $H_V$ ) and the fracture toughness coefficient ( $K_{FR}$ ) were measured using the Vickers indentation technique (EMCO-Test, DURA Scan-Operating system, Germany), subjected to various applied loads, ranging from 0.1 kg to 10 kg (broke limit) for 30 s with a  $136^\circ$  included peak angle (see Fig. 1). A diamond indenter in the form of a square-based pyramid was used.

## 3. Results and discussion

Fig. 2a shows the XRD patterns of the as-pressed samples. All the diffractions peaks are well-matched with the FeVSb HH phase

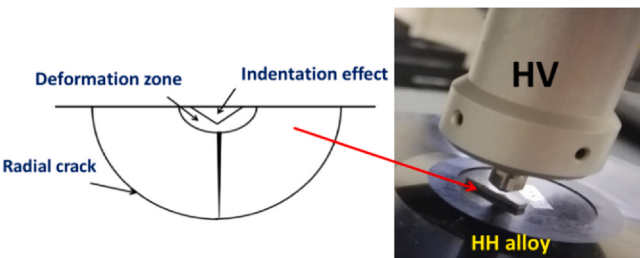


**Fig. 1.** Scheme for Vickers indentation technique.

(PDF#25-1134) as the dominant phase with a cubic MgAgAs-type crystal structure (space group  $F\bar{4} 3m$ ). The main peak shifting to the left side was observed, which suggests the successful substitution of host atom by dopants (see Fig. 2b). The lattice parameter ( $a$ ) increases with increasing doping level (see Table 1), showing good agreement with Vegard's law [13]. The obvious diversity of  $a$  values is mainly attributed to the difference between covalent radii of V ( $r_V = 1.53 \text{ \AA}$ ) and the doping elements Hf ( $r_{\text{Hf}} = 1.75 \text{ \AA}$ ), Ti ( $r_{\text{Ti}} = 1.60 \text{ \AA}$ ) and Nb ( $r_{\text{Nb}} = 1.64 \text{ \AA}$ ).

The SEM analysis are used to identify the microstructure and surface morphology after treating the samples with the SPS system and annealing processes (see Fig. 3b). SEM images of the  $\text{FeV}_{0.24}\text{Nb}_{0.4}\text{Hf}_{0.16}\text{Ti}_{0.2}\text{Sb}$  sample showed high densification of the sample, with no visible cracks or voids. The energy dispersive X-ray spectroscopy (EDX) result indicates that the elemental distribution is nearly uniform.

## 4. Thermoelectric properties

The transport thermoelectric properties of the samples were studied as a function of temperature from 300 to 800 K as shown in Fig. 4. The electrical conductivity of all the samples (except the  $\text{FeV}_{0.64}\text{Hf}_{0.16}\text{Ti}_{0.2}\text{Sb}$  compound) decreases with increasing temperature showing a metal-like conduction behaviour (see Fig. 4a). Value of the electrical conductivity at room temperature first decreased after the addition of doping elements, which is due to the mass defect caused by the large Hf ions [14], and then increased upon further doping. Such changes in the electrical conductivity are mainly ascribed to the dramatic enhancement in the charge carrier concentration upon doping (see Table 1). At 550 K,  $\text{FeV}_{0.9}\text{Hf}_{0.1}\text{Sb}$  sample showed the lowest electrical conductivity of  $3.7 \pm 0.3 \times 10^2 \Omega^{-1} \text{ cm}^{-1}$ , while the  $\text{FeV}_{0.24}\text{Nb}_{0.4}\text{Hf}_{0.16}\text{Ti}_{0.2}\text{Sb}$  sample exhibits the highest value of  $12 \pm 0.8 \times 10^2 \Omega^{-1} \text{ cm}^{-1}$  near room temperature.

Temperature dependence of Seebeck coefficient of  $\text{FeV}_{1-x-y-z}\text{Hf}_x\text{Ti}_y\text{Nb}_z\text{Sb}$  is shown in Fig. 4b. The Seebeck coefficient measurements indicated that the parent FeVSb sample is an n-type material. The Seebeck coefficient changes from negative to positive upon doping. Such result is attributed to the fact that Hf and Ti has one less electron than V, which increases the number of holes [15]. These explanations are in a good agreement with the results obtained by Hall coefficient measurements shown in Table 1. The maximum Seebeck coefficient was obtained for  $\text{FeV}_{0.24}\text{Nb}_{0.4}\text{Hf}_{0.16}\text{Ti}_{0.2}\text{Sb}$  sample with a value of  $147 \mu\text{V K}^{-1}$  at  $\sim 800$  K, which is higher than that reported by R. Hasan et al. for single doped  $\text{FeV}_{1-x}\text{Ti}_x\text{Sb}$  [16] and Young et al. [8]. By applying the formula proposed by Goldsmid and Sharp  $E_g = -2e|S_{\max}|T_{\max}$  [17], where  $E_g$  is the band gap,  $e$  the electronic charge, and  $T_{\max}$  the absolute temperature at which  $S_{\max}$  occurs, the calculated  $E_g$  for the FeVSb compound is about 0.13 eV, and  $E_g$  for the substituted samples is in the range of 0.13–0.23 eV (see Table 2).

Fig. 4c represents the power factor  $PF$  of the examined samples, which was calculated using the equation  $PF = S^2\sigma$ . The power factor increases as the temperature increases reaching a maximum point and then decreases, except for the  $\text{FeV}_{0.24}\text{Nb}_{0.4}\text{Hf}_{0.16}\text{Ti}_{0.2}\text{Sb}$  compound, which shows increasing behaviour with temperature. This

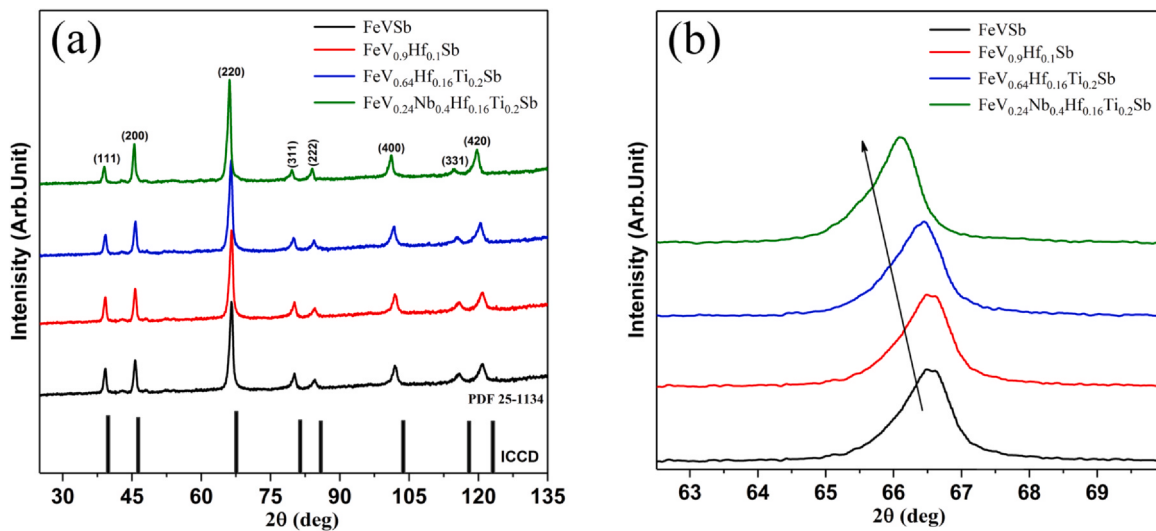


**Fig. 2.** (a) XRD patterns of  $\text{FeV}_{1-x-y-z}\text{Hf}_x\text{Ti}_y\text{Nb}_z\text{Sb}$  and (b) observed shift in the most intense peak (220) of the samples.

**Table 1**

Room-temperature Seebeck coefficient ( $S$ ), electrical conductivity ( $\sigma$ ), Hall coefficient ( $R_H$ ), carrier concentration ( $n$ ), carrier mobility ( $\mu$ ) and lattice parameters of the concerned samples.

Samples	$S$ ( $\mu\text{V K}^{-1}$ )	$\sigma$ ( $10^2 \Omega^{-1} \text{cm}^{-1}$ )	$R_H$ ( $\text{cm}^3 \text{C}^{-1}$ )	$n$ ( $10^{20} \text{cm}^{-3}$ )	$\mu$ ( $\text{cm}^2 \text{V}^{-1} \text{s}^{-1}$ )	$a$ ( $\text{\AA}$ )
FeVSb	$-110 \pm 5$	$7.5 \pm 0.5$	$-0.629$	$0.099$	$473$	$5.84$
FeV <sub>0.9</sub> Hf <sub>0.1</sub> Sb	$127 \pm 6$	$4.4 \pm 0.3$	$0.088$	$0.71$	$39$	$5.85$
FeV <sub>0.64</sub> Hf <sub>0.16</sub> Ti <sub>0.2</sub> Sb	$93 \pm 4$	$12 \pm 0.8$	$0.011$	$5.5$	$6.5$	$5.89$
FeV <sub>0.24</sub> Nb <sub>0.4</sub> Hf <sub>0.16</sub> Ti <sub>0.2</sub> Sb	$128 \pm 6$	$5.8 \pm 0.4$	$0.012$	$11.1$	$6.8$	$5.94$

can be ascribed to the behaviours of the Seebeck coefficient and the electrical conductivity. As a result, a maximum  $PF = 19.5 \pm 1.7 \mu\text{W cm}^{-1} \text{K}^{-2}$  was observed for the  $\text{FeV}_{0.24}\text{Nb}_{0.4}\text{Hf}_{0.16}\text{Ti}_{0.2}\text{Sb}$  compound at 800 K.

Fig. 5a shows the temperature dependence of the lattice thermal conductivity,  $\kappa_l$ . The value of  $\kappa_l$  was calculated as:  $\kappa_l = \kappa_t - \kappa_e$ , while  $\kappa_e$  was estimated from the well-known Wiedemann-Franz law as:  $\kappa_e = L\sigma T$ . Here  $L$  is the Lorenz number, which was estimated by using a single parabolic band model [12]. The numeric values of the Lorenz number are in the range of  $(1.65-2.1) \times 10^{-8} \text{ W}\Omega\text{K}^{-2}$ . The total thermal conductivity,  $\kappa_t$ , for all samples are plotted in the inset of Fig. 5a. Our previous study showed that at room temperature, a ~48% reduction in  $\kappa_l$  attained in FeVSb by the substitution of Hf for V, is due to the enhanced point defect scattering [18]. Among all the samples, the  $\text{FeV}_{0.24}\text{Nb}_{0.4}\text{Hf}_{0.16}\text{Ti}_{0.2}\text{Sb}$  compound has the lowest  $\kappa_l$  with a value of  $(1.81 \pm 0.1 \text{ W m}^{-1} \text{ K}^{-1})$  at room temperature with a

reduction of ~82% compared with that of FeVSb. This indicates that a large enhancement of alloy scattering for phonons, resulting from the mass fluctuation and the strain field fluctuation between the host atoms and the impurity atoms is an effective way to reduce  $\kappa_l$  of the FeVSb compound [19,20]. The  $\text{FeV}_{0.64}\text{Hf}_{0.16}\text{Ti}_{0.2}\text{Sb}$  sample showed the lowest thermal conductivity  $(2.3 \pm 0.1 \text{ W m}^{-1} \text{ K}^{-1})$ , which is ~78% less than that of the FeVSb sample  $(10.5 \pm 0.5 \text{ W m}^{-1} \text{ K}^{-1})$ .

The temperature dependence of the thermoelectric figure of merit  $zT$  of samples is shown in Fig. 5b. Generally,  $zT$  increased with increasing temperature, exhibits a maximum value of 0.44 at 725 K for the  $\text{FeV}_{0.24}\text{Nb}_{0.4}\text{Hf}_{0.16}\text{Ti}_{0.2}\text{Sb}$  compound. This enhancement with  $zT$  can be ascribed to the more significant improvement in power factor and suppression of the total thermal conductivity. Further improving the efficiency of thermoelectric materials could be achieved via doping strategy.

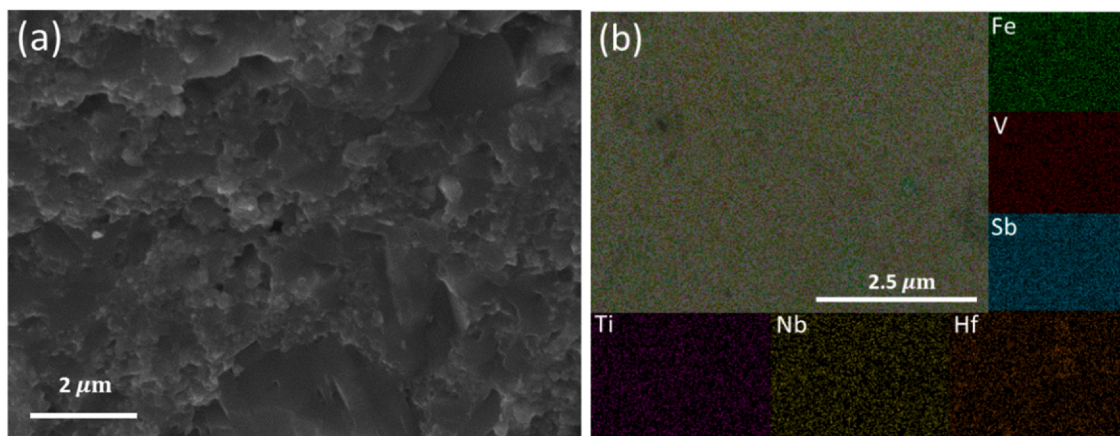


**Fig. 3.** (a) The SEM image of the fractured surface, (b) back-scattering image and EDX compositional mapping of the polished surface for the  $\text{FeV}_{0.24}\text{Nb}_{0.4}\text{Hf}_{0.16}\text{Ti}_{0.2}\text{Sb}$  sample.

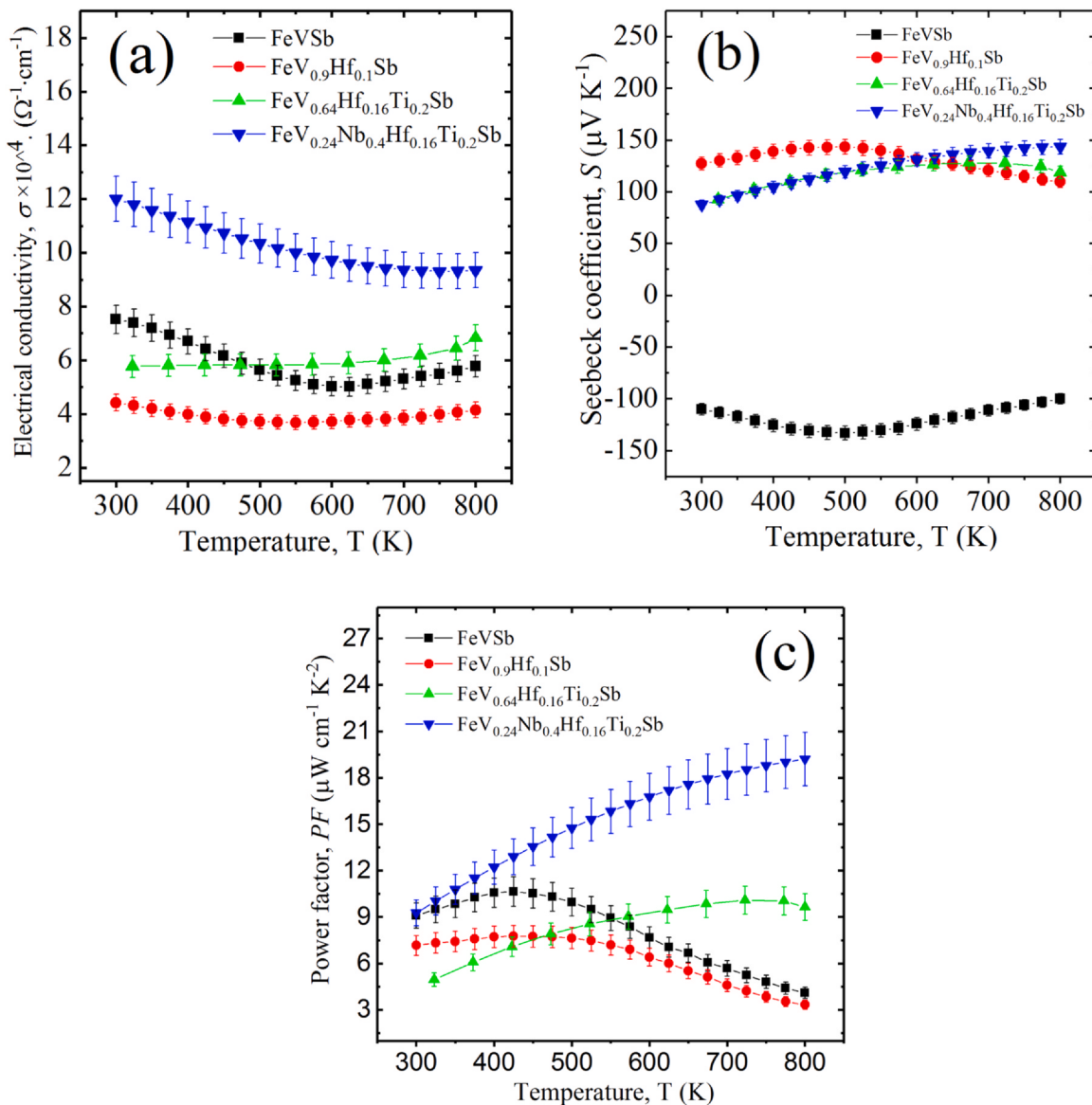


**Fig. 4.** Temperature dependence of the thermoelectric properties of  $\text{FeV}_{1-x-y-z}\text{Hf}_x\text{Nb}_x\text{Sb}$  samples; a) electrical conductivity, b) Seebeck coefficient and c) power factor.

**Table 2**

The relative density  $\rho$  (%), band gap ( $E_g$ ) and the Vickers hardness ( $HV$ ) data at high loads of the concerned compounds.

HH alloys compounds	$\rho$ (%)	$E_g$ (eV)	$HV_1$	$HV_5$
FeVSb	96.9	0.13	$6.87 \pm 0.27$	$6.18 \pm 0.25$
FeV <sub>0.9</sub> Hf <sub>0.1</sub> Sb	94.6	0.14	$7.33 \pm 0.29$	$6.89 \pm 0.28$
FeV <sub>0.64</sub> Hf <sub>0.16</sub> Ti <sub>0.2</sub> Sb	91.4	0.17	$8.17 \pm 0.33$	$7.83 \pm 0.31$
FeV <sub>0.24</sub> Nb <sub>0.4</sub> Hf <sub>0.16</sub> Ti <sub>0.2</sub> Sb	93.3	0.23	$8.05 \pm 0.32$	$6.75 \pm 0.27$

In terms of  $zT$  comparison, a  $zT$  value of 1.5 at 1200 K was recorded for p-type FeNbSb thermoelectric materials [7], while a maximum  $zT$  of 1.1 at 1100 K was obtained for p-type  $\text{FeNb}_{1-x}\text{Ti}_x\text{Sb}$  half-Heusler alloys [21]. On the other hand, the thermoelectric properties of NbFeSb and  $\text{Nb}_{0.85}\text{M}_{0.15}\text{FeSb}$  ( $M = \text{Ti}, \text{Zr}, \text{Hf}$ ) alloys were studied in the temperature range from 400 to 823 K. the studied samples showed low  $zT$  at 0.002 for the NbFeSb compound [22].

## 5. Mechanical properties

Mechanical properties are very important for TE applications [23]. We are looking for excellent mechanical properties of the

samples while maintaining high  $zT$  values. The  $HV$  for each sample was measured with a micro hardness technique (see Fig. 1). For all indentation data the hardness  $HV$  is

$$HV = 0.102 \times \frac{2F \sin^{136}}{(2a)^2} = 1.891 \frac{F}{(2a)^2} \quad (1)$$

where  $2a$  is the diagonal length of the indent and  $F$  is the indentation load. The value of  $HV$  has been found to be a function of the applied indentation load for a variety of materials. In this study, the concerned samples with different doping were indented under a sequence of loads (0.98 N, 4.9 N, 9.8 N and 49 N), which labeled as ( $HV_{0.1}$ ,  $HV_{0.5}$ ,  $HV_1$ ,  $HV_5$ ). It is obvious that the calculated  $HV$  values decrease as the applied load increases (see Fig. 6). At high loads (9.8 N and 49 N), no significant difference between  $HV$  values is observed (see Table 2). As a result,  $6.99 \pm 0.27$  GPa,  $9.33 \pm 0.37$  GPa,  $13.24 \pm 0.53$  GPa and  $19.15 \pm 0.77$  GPa were obtained for undoped (FeVSb), single doped (FeV<sub>0.9</sub>Hf<sub>0.1</sub>Sb), double doped (FeV<sub>0.64</sub>Hf<sub>0.16</sub>Ti<sub>0.2</sub>Sb), triple doped (FeV<sub>0.24</sub>Nb<sub>0.4</sub>Hf<sub>0.16</sub>Ti<sub>0.2</sub>Sb) samples, respectively at load of 0.98 N. The indentation hardness in GPa (force per contact area under load) can be estimated as multiplied by 0.009806.

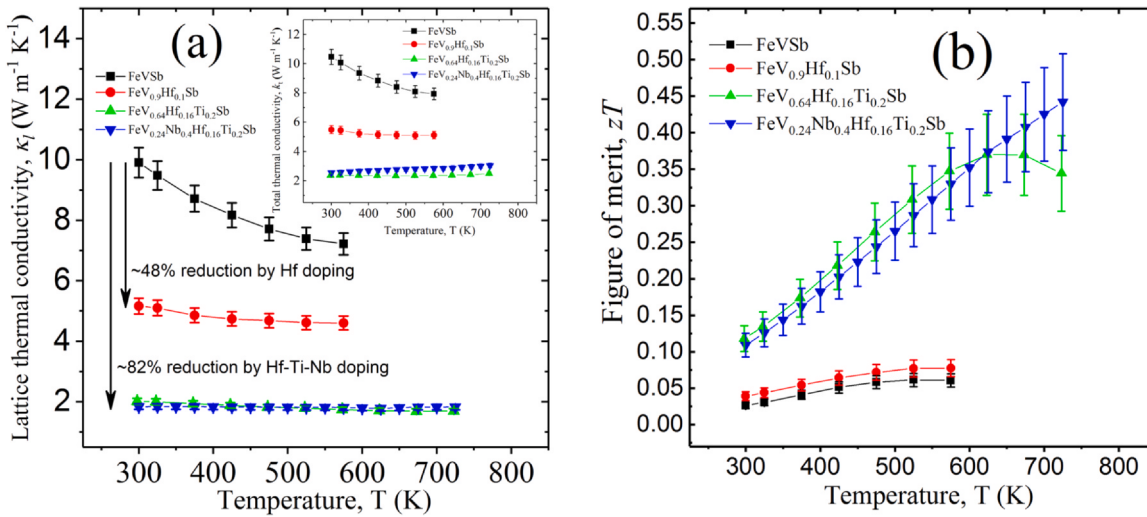


**Fig. 5.** Temperature dependences of: (a) lattice thermal conductivity and (b) the thermoelectric figure of merit for the  $\text{FeV}_{1-x-y-z}\text{Hf}_x\text{Ti}_y\text{Nb}_z\text{Sb}$  system. The inset in (a) is the measured total thermal conductivity.

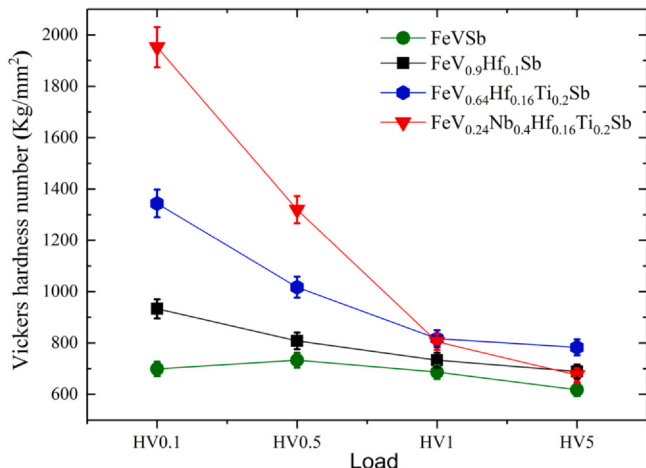


**Fig. 6.** Vickers hardness number as a function of different indentation load.

The fracture toughness resistance ( $K_{FR}$ ) estimated by applying the Shetty-equation [24].

$$K_{FR} = 0.0675 \sqrt{\frac{a^2}{c-a}} \quad (HV) \quad (2)$$

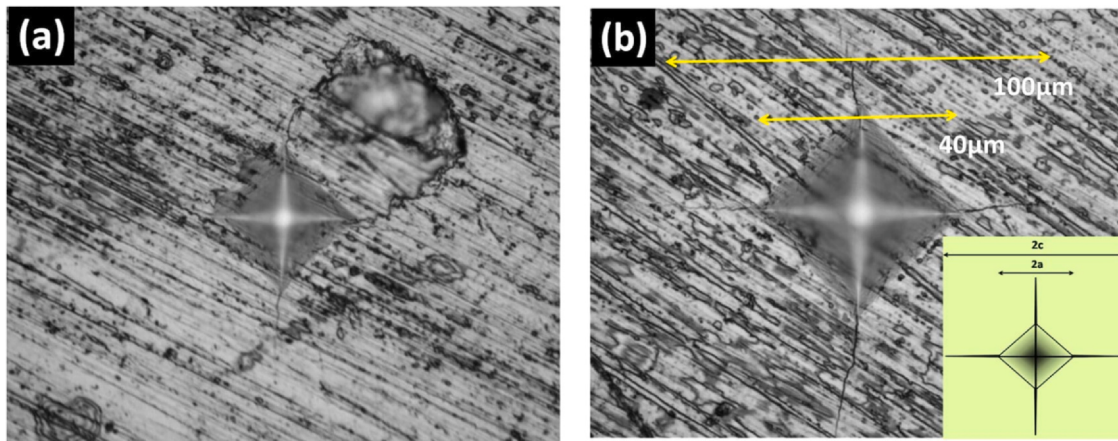


**Fig. 7.** Photomicrographs of the  $\text{FeV}_{0.24}\text{Nb}_{0.4}\text{Hf}_{0.16}\text{Ti}_{0.2}\text{Sb}$  compound showing the locations of Vickers indentation hardness notions and the crack outlines at two different loads: (a) 9.8 N and (b) 49 N.

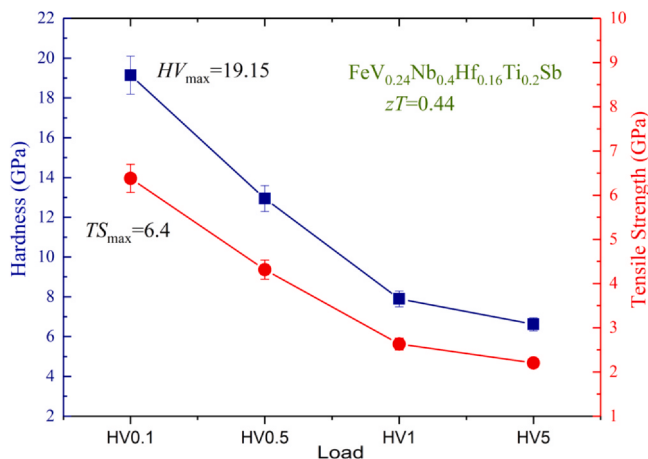


**Fig. 8.** Hardness and Tensile strength with different indentation load for  $\text{FeV}_{0.24}\text{Nb}_{0.4}\text{Hf}_{0.16}\text{Ti}_{0.2}\text{Sb}$ .

## 6. Conclusion

The concerned alloys were successfully synthesized by arc/induction melting followed by mechanical alloying (MA) and treated with the spark plasma sintering (SPS) system. The power factor significantly increased, whereas a reduction in the thermal conductivity was achieved with increasing doping content. A dramatic reduction of ~82% at room temperature in the FeVSb lattice thermal conductivity was obtained due to point defect scattering introduced by Hf-Ti-Nb triple-doping. Vickers method is extremely accurate to calculate the hardness value of alloys. The  $\text{FeV}_{0.24}\text{Nb}_{0.4}\text{Hf}_{0.16}\text{Ti}_{0.2}\text{Sb}$  compound showed the highest  $zT$  of 0.44 has been obtained at 725 K,  $HV$  with value of  $19.15 \pm 0.75$  GPa and  $TS$  of  $6.4 \pm 0.25$  GPa at load of 0.98 N.

## Declaration of Competing Interest

The authors declare that they have no known competing financial interests or personal relationships that could have appeared to influence the work reported in this paper.

## Acknowledgements

The work at NUST “MISiS” was supported by the Russian Science Foundation (project No. 21-12-00405). This work was funded through Researchers Supporting Project number (RSP-2021/79) at King Saud University, Riyadh, Saudi Arabia.

## References

- [1] A.M. Adam, A. El-Khouly, A.K. Diab, Effects of transition metal element doping on the structural and thermoelectric properties of n-type  $\text{Bi}_{2-x}\text{Ag}_x\text{Se}_3$  alloys, *J. Alloys Compd.* 851 (2021) 156887.
- [2] A.M. Adam, A. El-Khouly, A.P. Novitskii, E.M.M. Ibrahim, A.V. Kalugina, D.S. Pankratova, A.I. Taranova, A.A. Sakr, A.V. Trukhanov, M.M. Salem, Enhanced thermoelectric figure of merit in Bi-containing  $\text{Sb}_2\text{Te}_3$  bulk crystalline alloys, *J. Phys. Chem. Solids* 138 (2020) 109262.
- [3] A.M. Adam, E.M.M. Ibrahim, A. Panbude, K. Jayabal, P. Veluswamy, A.K. Diab, Thermoelectric power properties of Ge doped PbTe alloys, *J. Alloys Compd.* 872 (2021) 159630, <https://doi.org/10.1016/j.jallcom.2021.159630>
- [4] Y. Pei, X. Shi, A. LaLonde, H. Wang, L. Chen, G.J. Snyder, Convergence of electronic bands for high performance bulk thermoelectrics, *Nature* 473 (2011) 66–69.
- [5] H. Hohl, A.P. Ramirez, C. Goldmann, G. Ernst, B. Wölfling, E. Bucher, Efficient dopants for  $\text{ZrNiSn}$ -based thermoelectric materials, *J. Phys. Condens. Matter* 11 (1999) 1697–1709, <https://doi.org/10.1088/0953-8984/11/7/004>
- [6] M. Zou, J.-F. Li, T. Kita, Thermoelectric properties of fine-grained  $\text{FeVsB}$  half-Heusler alloys tuned to p-type by substituting vanadium with titanium, *J. Solid State Chem.* 198 (2013) 125–130.
- [7] C. Fu, S. Bai, Y. Liu, Y. Tang, L. Chen, X. Zhao, T. Zhu, Realizing high figure of merit in heavy-band p-type half-Heusler thermoelectric materials, *Nat. Commun.* 6 (2015) 8144, <https://doi.org/10.1038/ncommes9144>
- [8] D.P. Young, P. Khalifah, R.J. Cava, A.P. Ramirez, Thermoelectric properties of pure and doped  $\text{FeMSb}$  ( $M = \text{V}, \text{Nb}$ ), *J. Appl. Phys.* 87 (2000) 317–321.
- [9] Y. Huang, K. Hayashi, Y. Miyazaki, Electron conduction mechanism of deficient half-Heusler  $\text{VFesB}$  compound revealed by crystal and electronic structure analyses, *Chem. Mater.* 32 (2020) 5173–5181, <https://doi.org/10.1021/acs.chemmater.0c01189>
- [10] Y. Huang, K. Hayashi, Y. Miyazaki, Outstanding thermoelectric performance of n-type half-Heusler  $\text{Fe}(\text{Fe}_{1-x}\text{Co}_x)\text{Sb}$  compounds at room-temperature, *Acta Mater.* 215 (2021) 117022, <https://doi.org/10.1016/j.actamat.2021.117022>
- [11] B. Kong, B. Zhu, Y. Cheng, L. Zhang, Q.-X. Zeng, X.-W. Sun, Structural, mechanical, thermodynamics properties and phase transition of  $\text{FeVsB}$ , *Phys. B Condens. Matter* 406 (2011) 3003–3010, <https://doi.org/10.1016/j.physb.2011.04.067>
- [12] A. El-Khouly, A. Novitskii, I. Serhiienko, A. Kalugina, A. Sedegov, D. Karpenkov, A. Voronin, V. Khovaylo, A.M. Adam, Optimizing the thermoelectric performance of  $\text{FeVsB}$  half-Heusler compound via Hf-Ti double doping, *J. Power Sources* 477 (2020) 228768, <https://doi.org/10.1016/j.jpowsour.2020.228768>
- [13] A.R. Denton, N.W. Ashcroft, Vegard's law, *Phys. Rev. A* 43 (1991) 3161–3164, <https://doi.org/10.1103/PhysRevA.43.3161>
- [14] R. Stern, B. Dongre, G.K.H. Madsen, Extrinsic doping of the half-Heusler compounds, *Nanotechnology* 27 (2016) 334002.
- [15] R. Hasan, S.-C. Ur, Synthesis of tin-doped  $\text{FeVsB}$  half-Heusler system by mechanical alloying and evaluation of thermoelectric performance, *Trans. Electr. Electron. Mater.* 19 (2018) 106–111.
- [16] R. Hasan, S.-C. Ur, Thermoelectric and transport properties of  $\text{FeV}_{1-x}\text{Ti}_x\text{Sb}$  half-Heusler system synthesized by controlled mechanical alloying process, *Electron. Mater. Lett.* 14 (2018) 725–732.
- [17] H.J. Goldsmid, J.W. Sharp, Estimation of the thermal band gap of a semiconductor from Seebeck measurements, *J. Electron. Mater.* 28 (1999) 869–872.
- [18] A. El-Khouly, A. Novitskii, A.M. Adam, A. Sedegov, A. Kalugina, D. Pankratova, D. Karpenkov, V. Khovaylo, Transport and thermoelectric properties of Hf-doped  $\text{FeVsB}$  half-Heusler alloys, *J. Alloys Compd.* 820 (2020) 153413.
- [19] J. Yang, G.P. Meissner, L. Chen, Strain field fluctuation effects on lattice thermal conductivity of  $\text{ZrNiSn}$ -based thermoelectric compounds, *Appl. Phys. Lett.* 85 (2004) 1140–1142.
- [20] A. El-Khouly, A.M. Adam, A. Novitskii, E.M.M. Ibrahim, I. Serhiienko, A. Nafady, M.K. Kuzhanov, D. Karpenkov, A. Voronin, V. Khovaylo, Effects of spark plasma sintering on enhancing the thermoelectric performance of Hf-Ti doped  $\text{FeVsB}$  half-Heusler alloys, *J. Phys. Chem. Solids* 150 (2021) 109848.
- [21] C. Fu, T. Zhu, Y. Liu, H. Xie, X. Zhao, Band engineering of high performance p-type  $\text{FeNbSb}$  based half-Heusler thermoelectric materials for figure of merit  $zT > 1$ , *Energy Environ. Sci.* 8 (2015) 216–220, <https://doi.org/10.1039/c4ee03042g>
- [22] A. Tavassoli, F. Falilamani, A. Grytsiv, G. Rogl, P. Heinrich, H. Müller, E. Bauer, M. Zehetbauer, P. Rogl, On the Half-Heusler compounds  $\text{Nb}_{1-x}(\text{Ti},\text{Zr},\text{Hf})_x\text{FeSb}$ : phase relations, thermoelectric properties at low and high temperature, and mechanical properties, *Acta Mater.* 135 (2017) 263–276, <https://doi.org/10.1016/j.actamat.2017.06.011>
- [23] G. Rogl, A. Grytsiv, M. Gürth, A. Tavassoli, C. Ebner, A. Wünschek, S. Puchegger, V. Sopranyuk, W. Schranz, E. Bauer, Mechanical properties of half-Heusler alloys, *Acta Mater.* 107 (2016) 178–195.
- [24] D.K. Shetty, I.G. Wright, P.N. Mincer, A.H. Clauer, Indentation fracture of WC-Co cermets, *J. Mater. Sci.* 20 (1985) 1873–1882.
- [25] E.E. Madeiros, A.M.S. Dias, Experimental and numerical analysis of Vickers hardness testing, *Int. J. Res. Rev. Appl. Sci.* 17 (2013) 9–18.
- [26] M.A. Verges, P.J. Schilling, P. Upadhyay, W.K. Miller, R. Yaqub, K.L. Stokes, P.F.P. Poudeu, Young's Modulus and Hardness of  $\text{Zr}_0.5\text{Hf}_0.5\text{Ni}_x\text{Pd}_{1-x}\text{Sn}_0.99\text{Sb}_0.01$  Half-Heusler Compounds, *Sci. Adv. Mater.* 3 (2011) 659–666.
- [27] M. Gürth, G. Rogl, V.V. Romaka, A. Grytsiv, E. Bauer, P. Rogl, Thermoelectric high  $ZT$  half-Heusler alloys  $\text{Ti}_{1-x-y}\text{Zr}_x\text{Hf}_y\text{Ni}_x\text{Sn}_{(0 \leq x \leq 1; 0 \leq y \leq 1)}$ , *Acta Mater.* 104 (2016) 210–222.